NANO COBALT FERRITE FOR THE REMOVAL OF TRIVALENT RARE EARTH ELEMENTS - ADSORPTION ISOTHERMS AND KINETICS

Sudha Thotakura, Anantha Lakshmi Vadivelu, Padmakar Rao Gogada, Lakshmi Bavisetti and Suryakala Duvvuri*

Department of Chemistry, GITAM School of Science, GITAM (Deemed to be University), Visakhapatnam, Andhra Pradesh, **INDIA.**

ABSTRACT:

In order to recycle rare earth cations (La^{3+} and Ce^{3+}) from aqueous solutions, $CoFe_2O_4$ magnetic nanoparticles are applied for the adsorption of trivalent lanthanum and cerium. Their adsorption isotherms, kinetics, and thermodynamics are comprehensively investigated. The adsorption followed pseudo second order kinetics and experimental data fitted using the Langmuir isotherm model. The optimal adsorption efficiency could be observed over 99% at neutral pH, indicating that nano spinel cobalt ferrite has a superior adsorption behavior at neutral and weak alkaline conditions. At room temperature, the maximum adsorption capacity is observed by the nanocrystalline $CoFe_2O_4$ is in the order of La (48.22 mg/g), and Ce (46.56 mg/g), respectively.

INTRODUCTION

Magnetic nanoparticles are very popular advanced materials[1,2] The possibility to guide these particles magnetically to recover them from solution by a magnet and to functionalize their surface with a large variety of functional groups has led to their application in biomedicine, homogeneous catalysis, wastewater processing and many other technological fields[3,4] . Here magnetic cobalt ferrite nanoparticles ($CoFe_2O_4$) were synthesized using co-precipitation method was applied for the adsorption of trivalent rare earth elements.

Rare earth elements (REE) consist of 15 lanthanides, scandium and yttrium [5]. They have important features in a wide diversity of special applications such as magnets [6], batteries [7], and telecommunications [8]. Based on their peculiar optical, chemical and metallurgical properties, the global demand for REE has increased more than 15% from 126,500 metric tons in 2010 to 196,000 metric tons in 2023. Although it is difficult to extract REEs due to their chemical similarities, there are several methods for this purpose comprising solvent extraction, fractional crystallization, chemical precipitation, adsorption and ion exchange[9].

The main reason for selecting La^{3+} and Ce^{3+} as the target cations is the fact that lanthanum and cerium constitute approximately 80% of REE global consumption [10] and, consequently, they are more abundant in the industrial wastewater. The major purpose of this work is to achieve a high-performance adsorbent for REE easy recycling from aqueous solutions.

Adsorption is considered as a fast, efficient, and inexpensive method for recovering/removing metals from aqueous solutions. Many authors have focused on the toxic elements removal [11,12]. However, prior investigations of REEs recovery from aqueous solutions using adsorption technology are limited.

MATERIALS AND METHODS
Materials:
a. Magnetic nano cobalt ferrite powder
b. Sulphuric acid (H_2SO_4)
c. Hydrochloric acid (HCl)
d. Sodium hydroxide (NaOH)
e. Lanthanum nitrate ($La(NO_3)_3.6H_2O$)
f. Cerium nitrate ($Ce(NO_3)_3 \cdot 6H_2O$)

All the reagents were of analytical grade and were purchased from Sigma-Aldrich and the solutions were prepared using deionized (DI) water (18.2 MΩ.cm).

3460

Adsorption experiments

Adsorption experiments were generally carried out by shaking (250 rpm) the tubes containing 0.30 g/L well-dispersed MNP (sonicated for 5 min) and 100.0 mL solution of REE at different reaction times. The pH was adjusted using 0.1 M H_2SO_4 or NaOH aqueous solutions and maintained at reasonably constant value by repeated pH measurements and adjustments. The effects of pH (3.0–9.0), adsorption isotherms (REE initial concentration 50–500 mg/L), kinetics (5–120 min) and thermodynamics (298, 313 and 333 K) were studied. Agilent 7500 inductively coupled plasma atomic emission spectrometry (ICPAES) is used for the measurement of initial and final concentration of rare earth elements. Each reaction was conducted in triplication and the averaged results were reported. The element uptake rate of q_e (mg/g) was determined by the following equation.

$$q_e = \frac{(C_o - C_e)V}{m}$$

where C_0 and C_e are the REEs concentration in liquid phase at the initial and at time t (mg/L), respectively; m is the adsorbent amount (g); V is the volume used in the adsorption process (L). The potential use of these nanoparticles as adsorbent [13] for the removal of lanthanum and cerium from wastewater was investigated particularly[14]. For this purpose, the influence of pH, contact time and initial dose on the

sorption capacity of $CoFe_2O_4$ has been studied. The investigations for the pseudo second order kinetic model for the surface adsorption explained the adsorption kinetics most effectively. This involves chemisorption, where the removal from a solution is due to physicochemical interactions between the two phases [15].

RESULTS AND DISCUSSION

Effect of pH

As an important factor, pH can significantly influence the interactions of adsorbent and adsorbate during adsorption process.The trends of REEs adsorption on $CoFe_2O_4$ at various pH are illustrated in Fig. 2(a). The results showed that REEs have very similar adsorption strategy at the ranges of pH investigated. When the pH ranges from 7 to 8, the REEs residue in solution reached a value close to 0 (lower than the detection limits) in 10 min, suggesting a rapid and complete recovery of REEs at these pH values[16]. To avoid the REEs(OH)$_3$ precipitation, the concentrations of REEs are generally controlled at <10 mg/L, even in the level of 0.1 mg/L. At pH > 8, the rare earth cations are gradually precipitated as oxide and hydroxide [17], thus the adsorption is significantly decreased. Therefore, pH = 7 was selected as optimum value in the following experiment.
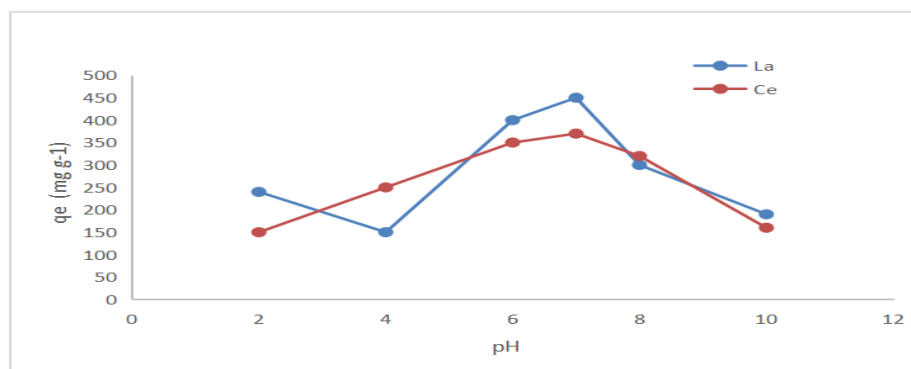

Figure 1: Effect of pH on trivalent lanthanum and cerium with cobalt ferrite

3461

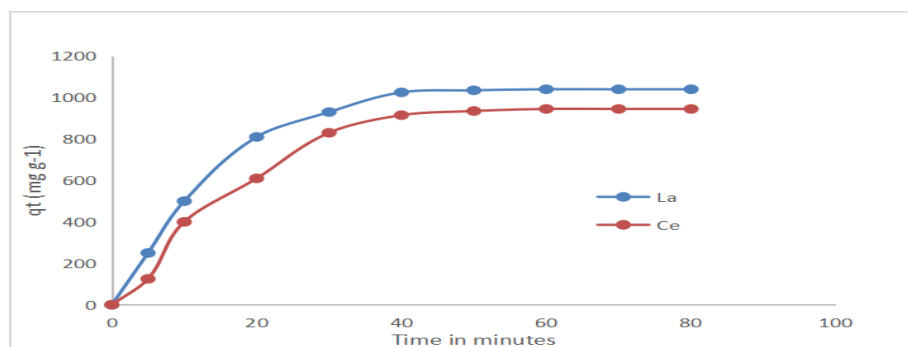Eur. Chem. Bull. 2023,12(Special issue 3), 3460 – 3466

Figure 2: Effect of contact time on trivalent lanthanum and cerium with cobalt ferrite

Adsorption kinetics and effect of contact time
The effect of contact time is shown in Fig. 2. The REE adsorption process was rapid at first (0–20 min) for all the three initial concentrations (100, 250 and 500 mg/g). As time progressed, the adsorption slowed down and finally reached equilibrium, which indicates that the adsorbents have fast kinetics[18].

Adsorption isotherms
Langmuir and Freundlich models are employed to study the adsorption isotherms. The Langmuir isotherm assumes that monolayer adsorption occurs on homogeneous surface and it has been commonly used to explain nano adsorbents behavior [19,20]. The Langmuir equation is defined as the following equation.

$$q_e = \frac{Q_{max}bC_e}{1+bC_e}$$

where Ce is the REE concentration at equilibrium (mg/L), q_e is the equilibrium adsorption capacity (mg/g), Qmax is the maximum capacity of the adsorbent (mg/g) and K_L is the Langmuir adsorption constant (L/ mg). K_L and q_m can be calculated from the linear fit of Ce/q_e versus Ce[21].

The Freundlich isotherm is an empirical equation that assumes surface sites, on which adsorption occurs, are heterogeneous [22,23]. The Freundlich equation is represented as the following equation.

$$q_e = K_F C_e^{1/n}$$

where K_F and n is the Freundlich constants and can be obtained from the linear fit of lnq_e versus lnCe [24].
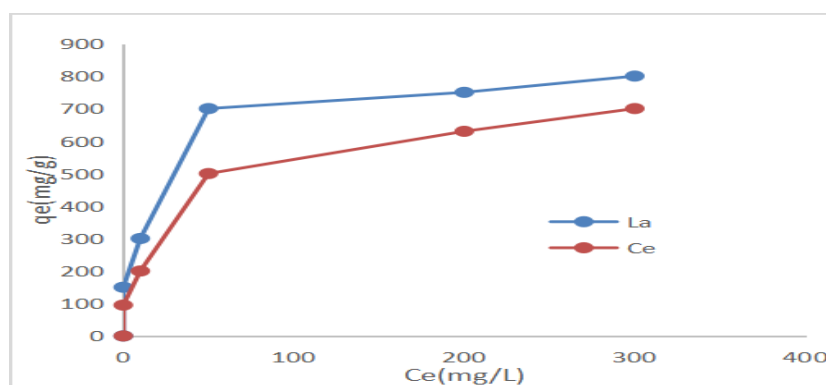

Figure 3: Equilibrium isotherms of REE; initial concentration of REE: 50–500 mg/L, adsorbent dosage: 0.3 g/L, volume of solution: 100 mL, time: 60 min, T: 298 K.

The adsorption isotherm data are shown in Fig. 3 and the results of the Langmuir, the Freundlich models are summarized in Table 1. The q_e becomes greater with increasing REE concentrations until reaching equilibrium. In

3462

addition, it can be seen that the experimental data of both La^{3+} and Ce^{3+} are more fitted with
.

the Langmuir model ($R^2 > 0.997$) and thus, the REE adsorption is monolayer

Table 1: Parameters of Langmuir and Freundlich adsorption isotherms

PAH	Parameters of Langmuir isotherm model			Parameters of Freundlich isotherm model		
	Q_{max} $\mu g\ g^{-1}$	b $L\mu g^{-1}$	r^2	K_F $\mu g\ g^{-1}$	1/n	r^2 g μg^{-1} m^{-1}
La	78.44	0.021	0.968	0.238	0.235	0.868
Ce	96.02	0.022	0.954	0.328	0.207	0.908

The maximum capacity (Q_{max}) of $CoFe_2O_4$ (La = 1001 and Ce = 982 mg/g) is significantly higher . On the other hand, Q_{max} for La^{3+} and Ce^{3+} is approximately equal, which can be attributed to their ionic radius closeness (La^{3+} =

1.061 Å and Ce^{3+} = 1.034 Å) [25]. Moreover, E values are between 8 and 16 kJ/mol, which demonstrate a chemical adsorption based on ion-exchange mechanism.

Table 2: Adsorption kinetics and parameters (Initial concentration is 100mg/L)

Trivalent REE	Parameters of pseudo first order kinetics				Parameters of pseudo second order kinetics			
	q_e (exp) mg g^{-1}	q_e (cal) mg g^{-1}	k_1 (min^{-1})	r^2	q_e (exp) mg g^{-1}	q_e (cal) mg g^{-1}	k_2 g mg^{-1} m^{-1}	r^2
La	28.12	35	0.074	0.795	335	334	1.54	0.954
Ce	68.36	83	0.088	0.898	283	284	1.08	0.966

Adsorption kinetics

This was investigated by pseudo-first order and pseudo-second order models [26,27], which are described in the respectively in the following equations.

$$q_t = q_e . e^{-k_1 t}$$

$$q_t = \frac{tq_e^2 k_2}{1 + tq_e k_2}$$

where qt (mg/g) represents the adsorption at time t (min), qe (mg/g) is the adsorption capacity of adsorbent at equilibrium, and k_1 (1/min) and k_2 (g/mg/min) are the pseudo-first order and the pseudo-second order kinetic rate constants, respectively. As listed in Table 3, the correlation coefficients (R^2) for the pseudo-second order model are higher than for the pseudo-first order model. Therefore, the experimental data are well described by pseudo-second order kinetics model ($R^2 > 0.999$), and the adsorption rate is controlled by chemical sorption [28,29].

Adsorption thermodynamics and effect of temperature

The thermodynamic studies are necessary for the practical applications. In order to investigate the effect of temperature on the changes in K_L value and thermodynamic parameters, the Gibbs free energy and the Van't Hoff equation were used [30,31].

$\Delta G° = \Delta H° - T\Delta S°$

Here $\Delta G°$ is the changes in Gibbs free energy, R is the ideal gas constant (8.314 J/mol/K), T is the absolute temperature (K), K_L is the Langmuir constant (L/mol), $\Delta H°$ and $\Delta S°$ are the changes in enthalpy and entropy, respectively. As listed in Table 3, the negative values of $\Delta G°$ imply that all the adsorption processes are spontaneous[32,33]. Furthermore, at higher temperature, $\Delta G°$ is more negative, which indicates that the temperature rising causes more efficient adsorption is confirmed in Fig.3. On the other hand, the adsorption processes are endothermic due to the positive values of $\Delta H°$, and the low positive values of $\Delta S°$ demonstrate that the randomness is

moderately increased during the adsorption procedure [34,35].

The adsorption capacities of REE ions onto specific adsorbent is summarized. The .

comparison obviously shows that $CoFe_2O_4$ MNP has high adsorption capacity and can be used as a high-performance adsorbent for REE ions[36,37]
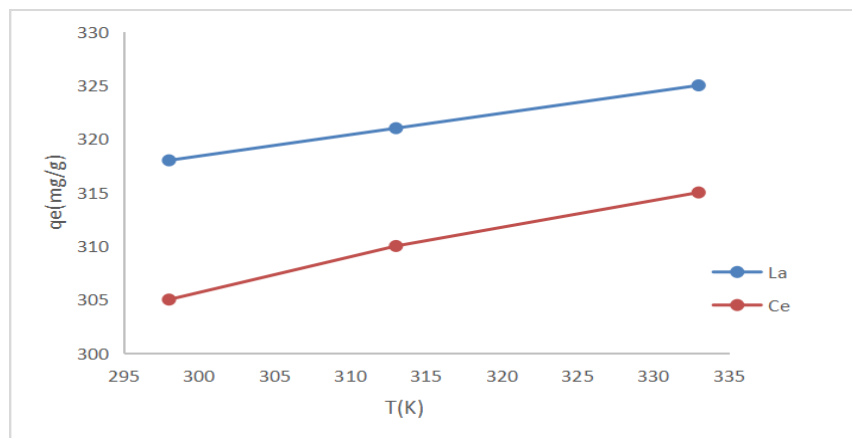

Figure 3: Effect of temperature on adsorption of trivalent La and cerium on cobalt ferrite magnetic nano particles.

Table 3: Thermodynamic parameters of trivalent rare earth elements

Trivalent rare earth element	ΔG^0			ΔS^0	ΔH^0
	298K	313K	333K		
Lanthanum	-8.64	-8.45	-9.85	0.036	2.96
Cerium	-8.54	-9.08	-9.78	0.046	2.05

From Table 3, clearly a close agreement among the experimental values and corresponding pseudo-second order kinetic model is observed [38,39].

CONCLUSION

Result of this study explains , low cost spin shaped cobalt ferrite nano particles using the co-precipitation method were applied as sorbent for removal of rare earth elements. These spinel ferrites were found to be efficient for the removal of REE namely lanthanum and cerium in their trivalent state. Optimum dosages of spinel ferrite for the removal of these REEs was found to be around 30 mg with generally neutral pH values resulting in higher removal efficiencies. The batch adsorption studies followed pseudo second order kinetics and thermodynamic studies are conducted. Therefore, spinel ferrite can be considered as a potential candidate in adsorption chemistry for removal of REEs from aqueous media.

CONFLICTS OF INTEREST
There are no conflicts to declare by the authors.

ACKNOWLEDGMENT

REFERENCES

1) Lu, A.-H.; Salabas, E. L.; Schüth, F. Magnetic Nanoparticles: Synthesis, Protection, Functionalization, and Application. Angew. Chem., Int. Ed. 2007, 46, 1222−1244.

2) Liu, Z.; Li, B.; Wang, B.; Yang, Z.; Wang, Q.; Li, T.; Qin, D.; Li, Y.; Wang, M.; Yan, M. Magnetic Nanoparticles Modified with DTPA AMC-Rare Earth for Fluorescent and Magnetic Resonance Dual Mode Imaging. Dalton Trans. 2012, 41, 8723−8728.

3) Wang, B.; Hai, J.; Wang, Q.; Li, T.; Yang, Z. Coupling of Luminescent Terbium Complexes to Fe3O4 Nanoparticles for Imaging Applications. Angew. Chem., Int. Ed. 2011, 50, 3063−3066.

4) Xi, P.; Cheng, K.; Sun, X.; Zeng, Z.; Sun, S. Magnetic Fe3O4 Nanoparticles Coupled with a Fluorescent Eu Complex for Dual Imaging Applications. Chem. Commun. 2012, 48, 2952−2954.

5) Goon, I. Y.; Zhang, C.; Lim, M.; Gooding, J. J.; Amal, R. Controlled Fabrication of Polyethylenimine-Functionalized Magnetic Nanoparticles for the Sequestration and Quantification of Free Cu2+. Langmuir 2010, 26, 12247−12252.

6) Liu, Y.; Chen, M.; Yongmei, H. Study on the Adsorption of Cu(II) by EDTA Functionalized Fe3O4 Magnetic Nano-Particles. Chem. Eng. J. 2013, 218, 46−54.

7) Ren, Y.; Abbood, H. A.; He, F.; Peng, H.; Huang, K. Magnetic EDTA-modified Chitosan/SiO2/Fe3O4 Adsorbent: Preparation, Char acterization, and Application in Heavy Metal Adsorption. Chem. Eng. J. 2013, 226, 300−311.

8) Sun, L.; Li, Y.; Sun, M.; Wang, H.; Xu, S.; Zhang, C.; Yang, Q. Porphyrin-Functionalized Fe3O4@SiO2 Core/Shell Magnetic Colori metric Material for Detection, Adsorption and Removal of Hg2+ in Aqueous Solution. New J. Chem. 2011, 35, 2697−2704.

9) Warner, C. L.; Addleman, R. S.; Cinson, A. D.; Droubay, T. C.; Engelhard, M. H.; Nash, M. A.; Yantasee, W.; Warner, M. G. High Performance, Superparamagnetic, Nanoparticle-Based Heavy Metal Sorbents for Removal of Contaminants from Natural Waters. ChemSusChem 2010, 3, 749−757.

10) Rossier, M.; Koehler, F. M.; Athanassiou, E. K.; Grass, R. N.; Aeschlimann, B.; Gunther, D.; Stark, W. J. Gold Adsorption on the Carbon Surface of C/Co Nanoparticles Allows Magnetic Extraction from Extremely Diluted Aqueous Solutions. J. Mater. Chem. 2009, 19, 8239−8243.

11) Rossier, M.; Koehler, F. M.; Athanassiou, E. K.; Grass, R. N.; Waelle, M.; Birbaum, K.; Gü nther, D.; Stark, W. J. Energy-Efficient Noble Metal Recovery by the Use of Acid-stable Nanomagnets. Ind. Eng. Chem. Res. 2010, 49, 9355−9362.

12) Yantasee, W.; Warner, C. L.; Sangvanich, T.; Addleman, R. S.; Carter, T. G.; Wiacek, R. J.; Fryxell, G. E.; Timchalk, C.; Warner, M. G. Removal of Heavy Metals from Aqueous Systems with Thiol Functionalized Superparamagnetic Nanoparticles. Environ. Sci. Technol. 2007, 41, 5114−5119.

13) Hao, Y.-M.; Man, C.; Hu, Z.-B. Effective Removal of Cu (II) Ions from Aqueous Solution by Amino-functionalized Magnetic Nanoparticles. J. Hazard. Mater. 2010, 184, 392−399.

14) Wu, D.; Sun, Y.; Wang, Q. Adsorption of Lanthanum (III) from Aqueous Solution Using 2-ethylhexyl Phosphonic Acid Mono-2-ethylhexyl Ester-Grafted Magnetic Silica Nanocomposites. J. Hazard. Mater. 2013, 260, 409−419.

15) Yang, S.; Zong, P.; Ren, X.; Wang, Q.; Wang, X. Rapid and Highly Efficient Preconcentration of Eu(III) by Core−Shell Structured Fe3O4@Humic Acid Magnetic Nanoparticles. ACS Appl. Mater. Interfaces 2012, 4, 6891−6900.

16) Li, Y.; Wu, J.; Qi, D.; Xu, X.; Deng, C.; Yang, P.; Zhang, X. Novel Approach for the Synthesis of Fe3O4@TiO2 Core-Shell Microspheres and their Application to the Highly Specific Capture of Phosphopeptides for MALDI-TOF MS Analysis. Chem. Commun. 2008, 564−566.

17) Tucker-Schwartz, A. K.; Farrell, R. A.; Garrell, R. L. Thiol−ene Click Reaction as a General Route to Functional Trialkoxysilanes for Surface Coating Applications. J. Am. Chem. Soc. 2011, 133, 11026− 11029.

18) De Palma, R.; Peeters, S.; Van Bael, M. J.; Van den Rul, H.; Bonroy, K.; Laureyn, W.; Mullens, J.; Borghs, G.; Maes, G. Silane Ligand Exchange to Make Hydrophobic Superparamagnetic Nano particles Water-Dispersible. Chem. Mater. 2007, 19, 1821−1831.

19) Larsen, B. A.; Hurst, K. M.; Ashurst, W. R.; Serkova, N. J.; Stoldt, C. R. Mono and Dialkoxysilane Surface Modification of Superparamagnetic Iron Oxide Nanoparticles for Application as Magnetic Resonance Imaging Contrast Agents. J. Mater. Res. 2012, 27, 1846−1852.

20) Bloemen, M.; Brullot, W.; Luong, T. T.; Geukens, N.; Gils, A.; Verbiest, T. Improved Functionalization of Oleic Acid-Coated Iron Oxide Nanoparticles for Biomedical Applications. J. Nanopart. Res. 2012, 14, 1100−1010.

21) Hermanson, G. T. In Bioconjugate Techniques, 2nd ed.; Hermanson, G. T., Ed.; Academic Press: New York, 2008; pp 562− 581.

22) Xie, F.; Zhang, T. A.; Dreisinger, D.; Doyle, F. A critical review on solvent

3465

Eur. Chem. Bull. 2023,12(Special issue 3), 3460 − 3466

extraction of rare earths from aqueous solutions. Miner. Eng. 2014, 56, 10−28.

23) Choppin, G. R.; Goedken, M. P.; Gritmon, T. F. The Complexation of Lanthanides by Aminocarboxylate Ligands - II. J. Inorg. Nucl. Chem. 1977, 39, 2025−2030.

24) Vander Hoogerstraete, T.; Onghena, B.; Binnemans, K. Homogeneous Liquid−Liquid Extraction of Rare Earths with the Betaine−Betainium Bis(trifluoromethylsulfonyl)imide Ionic Liquid System. Int. J. Mol. Sci. 2013, 14, 21353−21377.

25) Dugas, V.; Chevalier, Y. Surface Hydroxylation and Silane Grafting on Fumed and Thermal Silica. J. Colloid Interface Sci. 2003, 264, 354−361.

26) Mueller, R.; Kammler, H. K.; Wegner, K.; Pratsinis, S. E. OH Surface Density of SiO2 and TiO2 by Thermogravimetric Analysis. Langmuir 2002, 19, 160−165.

27) Cornell, R. M.; Schwertmann, U. The Iron Oxides: Structure, Properties, Reactions, Occurrences and Uses, 2nd ed.; Wiley-VCH: Weinheim, 2003; Chapter 10, pp 221−235.

28) Zhao, J.; Milanova, M.; Warmoeskerken, M. M. C. G.; Dutschk, V. Surface Modification of TiO2 Nanoparticles with Silane Coupling Agents. Colloids Surf., A 2012, 413, 273−279.

29) Brullot, W.; Reddy, N. K.; Wouters, J.; Valev, V. K.; Goderis, B.; Vermant, J.; Verbiest, T. Versatile Ferrofluids Based on Polyethylene Glycol Coated Iron Oxide Nanoparticles. J. Magn. Magn. Mater. 2012, 324, 1919−1925.

30) Anderson, D. R. In Analysis of Silicones; Smith, A. L., Ed.; Wiley Interscience: New York, 1974; p 10.

31) Kosmulski, M. pH-Dependent Surface Charging and Points of Zero Charge. II. Update. J. Colloid Interface Sci. 2004, 275, 214−224.

32) Kosmulski, M. pH-Dependent Surface Charging and Points of Zero Charge. III. Update. J. Colloid Interface Sci. 2006, 298, 730−741.

33) Kosmulski, M. Surface Charging and Point of Zero Charge; CRC Press: Boca Raton, FL, 2009.

34) Huang, X.; Schmucker, A.; Dyke, J.; Hall, S. M.; Retrum, J.; Stein, B.; Remmes, N.; Baxter, D. V.; Dragnea, B.; Bronstein, L. M. Magnetic Nanoparticles with Functional Silanes: Evolution of Well Defined Shells from Anhydride Containing Silane. J. Mater. Chem. 2009, 19, 4231−4239.

35) Witucki, G. L. A Silane Primer - Chemistry and Applications of Alkoxy Silanes. J. Coat. Technol. 1993, 65, 57−60.

36) Harrison, R. D.; Ellis, H. Book of Data; Longman: Edinburgh Gate, U.K., 1984; p 166.

37) Fadeev, A. Y.; McCarthy, T. J. Self-Assembly Is Not the Only Reaction Possible Between Alkyltrichlorosilanes and Surfaces: Monomolecular and Oligomeric Covalently Attached Layers of Dichloro- and Trichloroalkylsilanes on Silicon. Langmuir 2000, 16, 7268−7274.

38) Madadrang, C. J.; Kim, H. Y.; Gao, G.; Wang, N.; Zhu, J.; Feng, H.; Gorring, M.; Kasner, M. L.; Hou, S. Adsorption Behavior of EDTA-Graphene Oxide for Pb (II) Removal. ACS Appl. Mater. Interfaces 2012, 4, 1186−1193.

39) Diakonov, I. I.; Ragnarsdottir, K. V.; Tagirov, B. R. Standard Thermodynamic Properties and Heat Capacity Equations of Rare Earth Hydroxides:: II. Ce(III)-, Pr-, Sm-, Eu(III)-, Gd-, Tb-, Dy-, Ho.

3466

Eur. Chem. Bull. 2023,12(Special issue 3), 3460 − 3466